# Regulation of tubular recycling endosome biogenesis by the p53-MICALL1 pathway

YUKIE TAKAHASHI[1,2], CHIZU TANIKAWA[1], TAKAFUMI MIYAMOTO[1,4], MAKOTO HIRATA[1], GUANXIONG WANG[4], KOJI UEDA[3], TSUNEHIKO KOMATSU[2] and KOICHI MATSUDA[1,4]

[1]Laboratory of Molecular Medicine, Human Genome Center, Institute of Medical Science, The University of Tokyo, Tokyo; [2]Department of Hematology, Teikyo University Chiba Medical Center, Chiba; [3]Cancer Proteomics Group, Cancer Precision Medicine Center, Japanese Foundation for Cancer Research, Tokyo; [4]Laboratory of Clinical Genome Sequencing, Department of Computational Biology and Medical Sciences, Graduate School of Frontier Sciences, The University of Tokyo, Tokyo, Japan

Received February 18, 2017; Accepted June 23, 2017

DOI: 10.3892/ijo.2017.4060

**Abstract.** *p53*, one of the most frequently mutated genes in colon cancer, suppresses cancer development through transactivation of its targets. Herein, we conducted a comprehensive analysis of the p53 downstream pathway in colorectal cancer by using multi-omics analysis. Mass spectrometric analysis of HCT116 $p53^{+/+}$ and HCT116 $p53^{-/-}$ cells treated with adriamycin identified 124 proteins increased by DNA damage in a p53-dependent manner. Further screening using a cDNA microarray and the TCGA database revealed MICALL1 as a novel p53 target, and we identified functional p53 binding motifs located approximately 3000 base pairs upstream of the *MICALL1* gene. *MICALL1* expression was significantly decreased in colorectal cancer tissues with *p53* mutation compared with those without *p53* mutation. In response to DNA damage, MICALL1 co-localized with RAB8A and CD2AP at tubular recycling endosomes, whereas these proteins hardly localized at tubular recycling endosomes when *p53* or *MICALL1* expression was inhibited by siRNA. Our findings show that p53 regulates tubular recycling endosome biogenesis via transcriptional regulation of MICALL1, whose expression is frequently suppressed in colorectal cancer tissues.

## Introduction

*p53* is the tumor-suppressor gene most frequently mutated in various types of cancer. *p53* is activated in response to cellular stress, thus resulting in expression of many genes and antitumor effects through regulation of the cell cycle, apoptosis and senescence (1). However, not only cell cycle arrest and apoptosis but also other mechanisms, such as metabolic regulation, are essential for p53-mediated tumor suppression (2), thus suggesting the existence of unidentified p53 downstream pathways that play a crucial role in this process.

Colorectal cancer (CRC) is the third and second most common cause of cancer death in men and women, respectively, worldwide. The number of new cases and deaths in 2013 were estimated to be 1.6 million and 0.7 million, respectively (3). Moreover, the average age at diagnosis is decreasing (4). A multistep mutation mechanism drives normal colon mucosal cells toward CRC (5). Causal genes include the tumor-suppressor genes *adenomatous polyposis coli (APC), KRAS*, and *p53*. Initially, APC is inactivated, and this is followed by activating mutation of *KRAS*; *p53* mutation and loss of heterozygosity at chromosome 18q then induce early carcinoma. Accordingly, *p53* mutations have been found in 50-75% of CRC cases (6). In addition, *p53* mutations are significantly associated with poor prognosis (7,8). Therefore, identification of p53 targets in colorectal cancer cells is an important step in understanding the molecular pathogenesis of CRC.

In this study, we analyzed multi-omics data for HCT116 $p53^{+/+}$ and $p53^{-/-}$ colon cancer cell lines treated with Adriamycin and colon cancer data from the Cancer Genome Atlas Research Network (TCGA, https://tcgadata.nci.nih.gov/tcga/). Adriamycin was used for genotoxic stress to activate p53 in many cell lines including HCT116 cells in previous studies (9-11). Therefore, we used HCT116 cells and Adriamycin in this study. Our analyses identified MICALL1 (Molecule Interacting with CasL-like 1) as a novel p53 target. MICALL1, together with EHD1 and RAB8A, has been found to affect membrane tubulation of recycling endosomes (12). Herein, we explored the association between tubular recycling endosome biogenesis and the p53-MICALL1 pathway in the DNA damage response.

## Materials and methods

*Cell culture and treatment*. Human cancer cell lines HCT116 (colorectal adenocarcinoma) and H1299 (non-small cell lung

*Correspondence to:* Professor Koichi Matsuda, Laboratory of Clinical Genome Sequencing, Department of Computational Biology and Medical Sciences, Graduate School of Frontier Sciences, The University of Tokyo, 4-6-1 Shirokanedai, Minato-ku, Tokyo 108-8639, Japan
E-mail: koichima@ims.u-tokyo.ac.jp

*Key words:* p53, multi-omics, MICALL1, tubular recycling endosome, cell damage, colon cancer

cancer) were purchased from American Type Cell Collection (Rockville, MD, USA). HCT116 *p53*$^{+/+}$ and HCT116 *p53*$^{-/-}$ cells were gifts from Dr B. Vogelstein (Johns Hopkins University, Baltimore, MD, USA). Human embryonic kidney cells (HEK293T: a subclone of HEK293 cells engineered to express the SV40 large T antigen) were purchased from Riken Cell Bank (Ibaraki, Japan). Cells were incubated in a 37˚C incubator containing 5% $CO_2$. HEK293T cells were transfected with Fugene6 (Promega, Madison, WI, USA). Small interfering RNA oligonucleotides were purchased from Sigma Genosis (Woollands, TX, USA) and transfected with Lipofectamine RNAiMAX reagent (Invitrogen). We generated and purified replication-deficient recombinant viruses expressing p53 (Ad-p53) or LacZ (Ad-LacZ), as previously described (13). H1299 (*p53*-null) cells were infected with viral solutions at various multiplicities of infection (MOIs) and incubated at 37˚C until being harvested. HCT116 cells were treated with 2 $\mu$g/ml ADR for 2 h to induce genotoxic stress.

*Mass-spectrometry and proteome data*. HCT116 *p53*$^{+/+}$ or *p53*$^{-/-}$ cells were harvested at 12, 24, 48, or 72 h after adriamycin (ADR) treatment or no treatment as control. Cells were lysed in buffer [8 M urea, 50 mM HEPES-NaOH, pH 8.0], and proteins were reduced with 10 mM Tris (2-carboxyethyl) phosphine (Sigma-Aldrich, St. Louis, MO, USA) at 37˚C for 30 min, then subjected to alkylation with 50 mM iodoacetamide (Sigma-Aldrich) at 25˚C in the dark for 45 min. The proteins were then digested with immobilized trypsin (Thermo Fisher Scientific, Bremen, Germany) at 37˚C for 6 h. The resulting peptides were desalted with solid phase extraction (Oasis HLB $\mu$-elution plate, Waters Corp., Milford, MA, USA) and analyzed by mass spectrometer (Linear Trap Quadropole Orbitrap Velos mass spectrometry, Thermo Fisher Scientific) combined with liquid chromatography (UltiMate 3000 RSLC nano-flow HPLC system, DIONEX Corporation, Sunnyvale, CA, USA). The LC/MS spectra were searched against the Homo sapiens protein sequence database in SwissProt using proteome analysis software (Proteome Discoverer 1.4 software, Thermo Fisher Scientific); a false discovery rate of 1% was set for both peptide and protein identification filters. Differential peptide quantification analysis (label-free quantification analysis) for 10 samples was performed on the Expressionist Server platform (Genedata AG, Basel, Switzerland), as previously described (14). The fold change after ADR treatment was calculated with the following formula: f1 = Median peak intensity in [(*p53*$^{+/+}$ with ADR at 12, 24, 48, 72 h) / (Maximum peak intensity in (*p53*$^{+/+}$ and *p53*$^{-/-}$ without ADR and *p53*$^{-/-}$ with ADR at 12, 24, 48, 72 h) +1].

For the proteome analysis, we analyzed 47,534 peaks (derived from 22,276 genes) on the basis of the following criteria: fold induction >2 and p<0.05. Candidates demonstrating at least one peptide satisfying the criteria were included.

*cDNA microarray and transcriptome data*. Gene expression analysis was carried out using microarray kit (Sure print G3 Human GE 8x60 K microarray, Agilent Technology, Santa Clara, CA, USA) according to the manufacturer's protocol. Briefly, HCT116 *p53*$^{+/+}$ and *p53*$^{-/-}$ cells were treated with 2 $\mu$g/ml ADR and incubated at 37˚C until being harvested. Total RNA was isolated from the cells through standard protocols. Each sample was labeled and hybridized to array slides.

The fold change after ADR treatment was calculated with the following formula: f2 = Median expression of probe in (*p53*$^{+/+}$ with ADR at 12, 24, 48 h)/Maximum expression of probe in (*p53*$^{+/+}$ and *p53*$^{-/-}$ without ADR and *p53*$^{-/-}$ with ADR at 12, 24, 48 h).

In the transcriptome analysis, we filtered 62,976 peaks (derived from 24,220 genes) on the basis of the following criteria: fold induction >2 and p<0.05. Genes demonstrating at least one probe satisfying the criteria were included.

*TCGA analysis*. *MICALL1* expression and *p53* mutation status in colorectal tumor samples were obtained from the Cancer Genome Atlas (TCGA) project by using cBioPortal. The expression levels of four sample categories, normal tissues (n=41), tumor tissues (n=389), tumor tissues with wild-type p53 (n=149), and tumor tissues with mutant p53 (n=114), were compared using Mann-Whitney U tests. We filtered candidates on the basis of the following criteria: i) a median expression level of normal tissues higher than the median expression level of tumor tissues (p<0.05); ii) a median expression level of *p53* wild-type tumor tissues higher than the median expression level of *p53* mutant tumor tissues (p<0.05). All analyses were performed with the EZR program (15).

*Plasmid construction*. cDNA fragments of MICALL1 or CD2AP amplified with KOD-plus DNA polymerase (Toyobo, Osaka, Japan) were cloned into the pCAGGS expression vector. The primers used for amplification are shown in Table I.

*Quantitative real-time PCR*. Total RNA from human cell lines was extracted with RNeasy Plus Mini kit (Qiagen, Valencia, CA, USA) according to the manufacturer's protocol. Complementary DNAs were synthesized with Superscript III reverse transcriptase (Invitrogen). Quantitative real-time PCR was performed with SYBR Green Master Mix and a Light Cycler 96 (Roche, Basel, Switzerland). Primer sequences are shown in Table I. The PCR cycling condition were as follows: initial melting at 95˚C for 5 sec, followed by 45 cycles at 55˚C for 10 sec and 72˚C for 10 sec. Analysis of the melting curve for the primers was conducted to confirm the specificity of the PCR product.

*Western blot analysis*. Cells were harvested and lysed with RIPA buffer containing 1 mM PMSF, 0.1 mM DTT, and 0.1% Calbiochem Protease Inhibitor Cocktail Set III, EDTA-free (Merck Millipore, Darmstadt, Germany). The lysed samples were sonicated with a 30 sec on/30 sec off cycle for 15 min with a Bioruptor UCD-200 (Cosmobio, Tokyo, Japan). The cell lysates were centrifuged at 14,000 x g for 15 min and boiled after addition of SDS sample buffer (Bio-Rad, Hercules, CA, USA). Each sample was separated by SDS-PAGE and transferred to nitrocellulose membranes that were blocked using 5% skim milk (198-1-605, Wako Pure Chemical Industries, Tokyo, Japan). Membranes were incubated at 4˚C overnight with a mouse monoclonal anti-MICALL1 antibody (1:100, sc-398397, Santa Cruz Biotechnology, Santa Cruz, CA, USA), a rabbit monoclonal anti-CD2AP antibody (1:100, sc-9137, Santa Cruz Biotechnology), a rabbit monoclonal anti-FLAG antibody

Table I. Sequence of primers and oligonucleotides.

| siRNA | Sense | Antisense |
|---|---|---|
| siMICALL1-1 | GGACAAUGUCUUCGAGAAUTT | AUUCUCGAAGACAUUGUCCTT |
| siMICALL1-2 | CCACAAAGAAGGCCACCAATT | UUGGUGGCCUUCUUUGUGGTT |
| sip53 | GACUCCAGUGGUAAUCUACTT | GUAGAUUACCACUGGAGUCTT |
| siEGFP | GCAGCACGACUUCUUCAAGTT | CUUGAAGAAGUCGUGCUGCTT |
| **qPCR** | **Forward** | **Reverse** |
| *MICALL1* | TTGGAAGCCATGATCAAGAA | CCCTTCTTCTTGCCCTCAG |
| *β-actin* | CCCTGGAGAAGAGCTACGAG | TGAAGGTAGTTTCGTGGATGC |
| RE1 (ChIP) | GGAGACAGTCAAACTGGAACTTT | CCTTAATTCAGTGCTGTTTTGTTTT |
| **Cloning** | **Forward** | **Reverse** |
| MICALL1 | AAAGAATTCGGGGTCATGGCTGGGCCGCG | AAACTCGAGGCTCTTGTCTCTGGGGGACT |
| CD2AP | AAAGGTACCCCCAGCATGGTTGACTATATTG | AAACTCGAGAGAAGACAGGACAGCTTTTTTCA GCTTCTC |
| p53BS | AAACTCGAGGGAGACAGTCAAACTGGAACTTT | AAAGATATCCCTTAATTCAGTGCTGTTTTGTTTT |
| RE1mt | AGTTTTTAACTCCTG GCCTTGGCTCCC | AAAACAACCTGGGCAATATAGGGAGAC |
| RE2mt | CACTGTTCCTGGCCCCATTTCTTAATT | GCTAATACCTGTAATCCCAACACTTTG |

(1:2000, F7425, Sigma-Aldrich), a rat monoclonal anti-HA antibody (1:2000, 3F10, Sigma-Aldrich), a mouse monoclonal anti-p53 antibody (1:1000, DO-1, Santa Cruz Biotechnology), a mouse monoclonal anti-p21 antibody (1;100, OP64, Merck Millipore), or a mouse monoclonal anti-β-actin antibody (1:1000, AC-15, Abcam, Cambridge, MA, USA). Membranes were washed and probed with the secondary antibody conjugated to horseradish peroxidase against mouse, rabbit, or rat (all 1:30000, Santa Cruz Biotechnology, ref sc-2005, sc-2004 and sc-2006, respectively). Finally, proteins were visualized by chemiluminescent detection (Amersham ECL Western Blotting Detection Reagent (GE Health Care, Freiburg, Germany).

*Co-immunoprecipitation*. Protein-protein interactions were investigated by co-immunoprecipitation experiments. HA-tagged MICALL1 proteins and FLAG-tagged CD2AP proteins were expressed in HEK293T cells with Fugene6 (E2692, 30 $\mu$l per dish, Promega). The cells were harvested after 36 h of transfection and lysed for one hour with 0.5% NP40 buffer containing 50 mM Tris pH 7.4, 150 mM NaCl and protease inhibitor cocktail. Whole cell extracts were subjected to immunoprecipitation overnight with anti-Flag (Sigma-Aldrich) and anti-HA (Sigma-Aldrich) antibodies cross-linked to agarose beads at 4˚C. Endogenous protein interactions in HCT116 $p53^{+/+}$ cells were also assessed by immunoprecipitation experiments using an anti-MICALL1 antibody (Santa Cruz Biotechnology). HCT116 $p53^{+/+}$ cells were incubated in 100-mm dishes and treated with 2 $\mu$g/ml ADR. After incubation for 48 h, the cells were harvested and lysed for one hour with the same buffer cocktail described above. The samples were incubated overnight with a mouse anti-MICALL1 antibody at 4˚C. The exogenous and endogenous immunoprecipitates were separated by SDS-polyacrylamide gel electrophoresis (SDS-PAGE) and immunoblotted using antibodies against MICALL1 and CD2AP.

*Gene reporter assay*. A DNA fragment including two potential p53 binding sequences of MICALL1 was amplified and cloned into the pGL4.24 vector (Promega). For mutagenesis, point mutations were introduced with site-directed mutagenesis at the 4th and 14th nucleotides (C to T mutations) and the 7th and 17th nucleotides (G to T mutations) within the consensus p53 binding sequence (16). Reporter assays were performed using a Dual Luciferase Assay System (pGL3-promoter) (Promega) or Dual-Glo Luciferase Assay System (pGL4.24) (Promega), as previously described (17). The sequences of the primers used for amplification and site-directed mutagenesis are shown in Table I. Cells were not treated with Adriamycin in this experiment.

*Chromatin immunoprecipitation assay*. We carried out a Chromatin immunoprecipitation (ChIP) assay with an EZ-Magna ChIP G Chromatin Immunoprecipitation kit (Merck Millipore), per the manufacturer's protocol. H1299 cells ($1x10^6$ cells per samples) infected with Ad-p53 or Ad-LacZ at a MOI of 10 were cross-linked with 1% formaldehyde for 10 min, washed with PBS, and lysed using nuclear lysis buffer. The sample lysates were sonicated with a Bioruptor UCD-200 (CosmoBio), and DNA was sheared to 200-1000 base pair. Each sample was immunoprecipitated with an anti-p53 antibody (OP-40; Merck Millipore) or normal mouse IgG (sc-2025; Santa Cruz Biotechnology). Column-purified DNA was quantified by qPCR. Cells were not treated with Adriamycin in this experiment.

Table II. Candidates from mass spectrometry data.

| Protein | Fold induction | CST3 | 3.5 | IBTK | 2.5 | PSAT1 | 8155.1 |
|---|---|---|---|---|---|---|---|
| A2M | 4776.6 | CTSD | 2.3 | ICA1L | 2.2 | PSPH | 2.5 |
| AARS | 2.3 | DDB2 | 18.9 | IGHM | 29185.6 | RAC2 | 17334.9 |
| ACOT7 | 2.6 | DGKA | 733.0 | IKBIP | 2.2 | RAN | 3.8 |
| ACTC1 | 7529.5 | DHX9 | 22436.4 | INPP1 | 5.3 | RHOC | 3.2 |
| AK1 | 11361.7 | DOHH | 2.5 | ISG15 | 23278.4 | RNH1 | 2.1 |
| AKR1A1 | 12455.7 | EEF1A1 | 16457.0 | ISYNA1 | 2.6 | RRM2B | 1296.7 |
| ALDH1A3 | 2.3 | EIF4G2 | 3.0 | KIAA0284 | 1356.2 | S100A13 | 9890.4 |
| ALDOA | 2.9 | EPPK1 | 130023.0 | KRT1 | 2.7 | S100A2 | 4.5 |
| ANXA4 | 11.6 | EPS8L2 | 30581.1 | KRT15 | 3534.4 | S100A6 | 2.2 |
| APOB | 2744.6 | FABP5 | 2.1 | KRT20 | 1590.2 | SARS | 6.6 |
| APOBEC3C | 5.9 | FAM129B | 3.1 | KRTAP2-2 | 14236.0 | SEC31A | 3710.3 |
| APOC3 | 3.2 | FAS | 2.5 | LARS | 2.4 | SERPINB1 | 2.4 |
| ARF5 | 3.1 | FBXO2 | 3.5 | LGALS3BP | 2.9 | SERPINB5 | 13228.3 |
| ARVCF | 2032.4 | FCN3 | 14826.8 | MAP1S | 527.0 | SERPINE1 | 2.7 |
| ASS1 | 4130.2 | FDXR | 2870.3 | MDM2 | 2628.4 | SFN | 3.3 |
| BLVRB | 12875.3 | FGA | 4701.4 | MICALL1 | 3.3 | SNX2 | 2.5 |
| C12orf23 | 2.3 | FLNA | 17199.7 | NPEPPS | 1289.0 | STAT1 | 3.8 |
| C4BPA | 3.5 | FLNC | 15972.6 | NSF | 4200.4 | STAT3 | 5728.8 |
| CA2 | 820.7 | FN1 | 163688.8 | NTPCR | 11802.5 | TERF2IP | 4.7 |
| CAPG | 2.8 | FSCN1 | 3780.2 | NUP54 | 2.3 | TIGAR | 7.0 |
| CASP8 | 2.7 | GAA | 875.9 | OPTN | 1665.6 | TKT | 2.5 |
| CCNDBP1 | 2.8 | GAST | 4742.3 | OR1E2 | 2942.6 | TOP1 | 481.2 |
| CDKN1A | 33800.2 | GDF15 | 19719.2 | PEPD | 2.2 | TP53 | 82559.3 |
| CEACAM1 | 2916.0 | GSS | 3.3 | PIR | 5.0 | TP53I3 | 68584.0 |
| CFL1 | 2.1 | GSTP1 | 4.2 | PML | 4518.9 | TUBA1A | 6062.4 |
| CLTC | 2.7 | HADHA | 2.5 | PNP | 6.3 | UBE2L6 | 2432.5 |
| CMBL | 3.6 | HARS | 15435.0 | PODXL | 4.5 | UMPS | 4894.2 |
| CMPK1 | 2.2 | HEBP1 | 2.5 | PPM1A | 2.1 | VWF | 76930.1 |
| COPG1 | 1078.7 | HLA-B | 2.4 | PRDX1 | 1088.3 | YWHAB | 2.4 |
| CRIP2 | 2.7 | HSPA4L | 13458.7 | PRKRA | 2.1 | YWHAG | 6.5 |

*Immunocytochemistry*. HCT116 *p53*$^{-/-}$ or *p53*$^{+/+}$ cells were grown on cover glasses, transfected with Lipofectamine RNAiMAX (Thermo Fisher Scientific) for 36 h and fixed with 4% paraformaldehyde (163-20145-500 ml, Wako) for 10 min. The fixed cells were permeabilized with 0.2% Triton X100 in PBS (both from Sigma-Aldrich, ref X100-6X500ML and P4417-100TAB, respectively) for 5 min. Cells were blocked with blocking buffer [0.2% Triton X-100 and 3% BSA (bovine serum albumin, 001-000-162, Jackson Immunoresearch Laboratories, Inc., West Grove, PA, USA), in PBS 1X] for 1 h. After that, cells were incubated with mouse monoclonal anti-MICALL1 antibody (1:50, sc-398397, Santa Cruz Biotechnology) and rabbit monoclonal anti-CD2AP antibody (1:50, sc-9137, Santa Cruz Biotechnology) or rabbit monoclonal anti-RAB8A (1:200, #6975, Cell Signaling Technology) in staining solution (0.2% Triton X-100 and 3% BSA in PBS) for 2 h at room temperature. After washes with PBS, cells were incubated with a goat anti-mouse-Alexa Fluor 594- and a goat anti-rabbit-Alexa Fluor 488-labeled secondary antibodies (both 1:2000, from Thermo Fisher Scientific, ref A-11008 and A-11005), prepared in staining solution for 1 h at room temperature. Nuclei were stained with DAPI (H1200, Vector Laboratories, Youngstown, OH, USA) for 25 min and visualized with FluoView FV1000 confocal microscope (Olympus, Tokyo, Japan).

*Colony formation assay*. HCT116 cells were plated at $1x10^4$ cells per 35-mm culture well one day before transfection with MICALL1. On the second day after transfection, the culture medium was replaced by one containing 0.5 mg/ml G418 (G-418 Sulfate, 070-05183, Wako) every 2 days. Surviving colonies were fixed with methanol and stained with 1% crystal violet, and visible colonies were counted.

## Results

*Induction of MICALL1 by cellular stress*. To identify novel p53 targets that play important roles in colorectal carcinogenesis, we previously performed transcriptome and proteome analyses using HCT116 *p53*$^{+/+}$ and *p53*$^{-/-}$ cells (18,19). After treatment with 2 $\mu$g/ml ADR for 2 h, cells were harvested at different time points; i.e., 12, 24, 48 and 72 h (72 h only

Table III. Candidates from microarray data.

| Gene | Fold induction | *COL2A1* | 25.2 | *GNAS* | 2.3 | *LOC390660* | 3.4 | *PRINS* | 4.5 | *SIGLEC14* | 14.1 |
|---|---|---|---|---|---|---|---|---|---|---|---|
| *ABCA1* | 15.6 | *CORO2A* | 2.3 | *GNMT* | 2.5 | *LOC440149* | 2.8 | *PRKX* | 2.1 | *SLC11A1* | 7.0 |
| *ABCA12* | 10.2 | *CRIP2* | 2.4 | *GPC5* | 3.9 | *LOC643401* | 3.8 | *PROC* | 2.6 | *SLC12A4* | 2.1 |
| *ABCA3* | 3.2 | *CRYBA1* | 3.6 | *GPR124* | 2.5 | *LOC643401* | 5.4 | *PRODH* | 9.2 | *SLC44A4* | 8.2 |
| *ABCB9* | 3.6 | *CSH1* | 4.2 | *GPR153* | 2.1 | *LOC643401* | 4.3 | *PROM2* | 10.2 | *SLC4A11* | 2.5 |
| *ABCD1* | 3.1 | *CST3* | 2.4 | *GPR56* | 2.8 | *LOC646268* | 3.5 | *PRSS56* | 2.2 | *SLC6A14* | 2.7 |
| *ABCG4* | 3.3 | *CST5* | 2.1 | *GPR87* | 7.5 | *LOC728978* | 25.9 | *PSAPL1* | 3.6 | *SLC7A10* | 4.3 |
| *ACER2* | 2.4 | *CSTA* | 2.5 | *GPRIN2* | 2.0 | *LOC729770* | 2.4 | *PSTPIP2* | 2.1 | *SLCO2B1* | 2.6 |
| *ACP5* | 2.2 | *CTAG1A* | 2.2 | *GRAP* | 2.1 | *LOC730227* | 5.1 | *PTAFR* | 4.9 | *SMTNL2* | 11.3 |
| *ACSL6* | 5.4 | *CXCL11* | 5.6 | *GRHL3* | 2.7 | *LOXL4* | 3.1 | *PTGES* | 2.3 | *SNAI3* | 6.4 |
| *ACTA2* | 12.4 | *CXCR2* | 5.1 | *GRID2IP* | 2.1 | *LPHN3* | 2.2 | *PTH1R* | 3.7 | *SORCS2* | 439.0 |
| *ADAMTS8* | 4.9 | *CXorf65* | 9.0 | *GRIN2C* | 10.1 | *LRP1* | 2.4 | *PTPRE* | 2.4 | *SPANXB2* | 2.1 |
| *ADCK3* | 2.9 | *CYFIP2* | 5.0 | *GRIN3B* | 4.6 | *LRP10* | 2.3 | *PTPRU* | 2.7 | *SPNS2* | 2.5 |
| *ADRB2* | 9.7 | *CYP4F12* | 2.2 | *H19* | 26.3 | *LSP1* | 7.9 | *PVRL4* | 9.9 | *SPNS3* | 2.3 |
| *AK1* | 2.2 | *CYP4F2* | 2.3 | *HAR1B* | 2.3 | *LY6D* | 6.5 | *PVT1* | 2.1 | *SPRY1* | 2.1 |
| *AKR1B10* | 27.4 | *CYP4F3* | 10.5 | *HEG1* | 2.1 | *LYL1* | 4.6 | *PXDN* | 3.7 | *SRGAP3* | 4.7 |
| *AKR1B15* | 22.0 | *DDB2* | 2.7 | *HES2* | 2.5 | *LYNX1* | 2.6 | *Q6TXG5* | 12.6 | *ST6GALNAC2* | 2.5 |
| *ALDH1L1* | 3.7 | *DDIT4* | 2.4 | *HES6* | 2.5 | *LYZL4* | 22.9 | *Q8E8P5* | 4.1 | *STARD10* | 2.1 |
| *ALOX5* | 31.2 | *DFNB31* | 2.4 | *HHAT* | 2.2 | *MAGEA11* | 2.7 | *RAB37* | 4.4 | *STAT4* | 2.6 |
| *AMOT* | 2.6 | *DGCR10* | 2.9 | *HLA-DQB1* | 2.5 | *MAST4* | 3.9 | *RABEPK* | 2.1 | *SULF2* | 29.0 |
| *ANKMY1* | 3.0 | *DIO3OS* | 2.2 | *HLA-DRB4* | 2.9 | *MBP* | 3.8 | *RALGDS* | 2.8 | *SULT1A2* | 2.1 |
| *ANKRD20A8P* | 2.3 | *DKFZp451A211* | 2.6 | *HLA-DRB5* | 2.5 | *MC1R* | 2.2 | *RASAL1* | 3.0 | *SV2A* | 2.1 |
| *ANKRD43* | 5.1 | *DLL1* | 2.2 | *HLA-DRB6* | 3.2 | *MDFI* | 2.0 | *RASGRF1* | 2.1 | *SYK* | 4.2 |
| *ANKRD58* | 2.3 | *DMBT1* | 5.0 | *HOGA1* | 2.2 | *MDM2* | 4.5 | *RASSF4* | 2.5 | *SYNM* | 2.5 |
| *ANKRD65* | 4.4 | *DNAH3* | 3.9 | *HOXB13* | 2.0 | *METTL7A* | 2.2 | *RD3* | 8.6 | *SYT12* | 2.2 |
| *ANKUB1* | 4.8 | *DPEP2* | 2.6 | *HRCT1* | 2.2 | *MFSD4* | 2.6 | *REEP2* | 4.0 | *SULT1A2* | 2.1 |
| *ANXA4* | 2.4 | *DPYSL4* | 12.4 | *HS3ST6* | 6.1 | *MFSD6L* | 2.8 | *RET* | 2.5 | *SV2A* | 2.1 |
| *ANXA8L2* | 5.3 | *DRAM1* | 2.7 | *HSD17B1* | 2.9 | *MGAT3* | 4.4 | *RGL1* | 3.2 | *SYK* | 4.2 |
| *APOBEC3C* | 3.9 | *DRD2* | 2.1 | *HSD17B7* | 2.1 | *MGC20647* | 17.5 | *RGS16* | 3.2 | *SYNM* | 2.5 |
| *APOBEC3F* | 4.0 | *DSC3* | 5.5 | *HSD3B1* | 9.4 | *MICALL1* | 3.2 | *RHOD* | 3.4 | *SYT12* | 2.2 |
| *APOBEC3H* | 6.9 | *DUOX1* | 4.4 | *HSD3B2* | 2.6 | *MLPH* | 2.1 | *RIC3* | 12.8 | *SYT8* | 3.9 |
| *APOC1* | 2.5 | *DUSP13* | 8.6 | *HSPB7* | 2.6 | *MOV10L1* | 2.3 | *RIIAD1* | 2.4 | *SYTL1* | 2.8 |
| *APOL2* | 2.2 | *DUSP26* | 4.2 | *HSPG2* | 2.8 | *MRPL23-AS1* | 8.1 | *RIMBP3* | 2.1 | *TAP1* | 3.9 |
| *AQP3* | 2.5 | *EBI3* | 4.0 | *HTRA1* | 2.5 | *MS4A15* | 2.3 | *RIMS4* | 3.1 | *TCERG1L* | 2.4 |
| *ARAP1* | 2.5 | *EDN2* | 10.1 | *HYAL1* | 2.7 | *MTMR9LP* | 2.6 | *RIN1* | 2.8 | *TCF15* | 2.1 |
| *ARVCF* | 5.1 | *EFCAB10* | 3.9 | *ICAM2* | 2.8 | *MX1* | 4.2 | *RINL* | 2.3 | *TDRD6* | 5.2 |
| *ARX* | 2.1 | *EFNB1* | 2.4 | *ICAM4* | 7.8 | *MYBPHL* | 22.1 | *ROM1* | 2.3 | *TFEC* | 2.4 |
| *ASS1* | 2.6 | *EIF2AK4* | 2.2 | *IFITM10* | 2.4 | *MYH16* | 4.4 | *ROR1* | 2.6 | *TGM5* | 2.3 |
| *ASTN2* | 3.0 | *EIF4E3* | 2.6 | *IGFBP3* | 15.9 | *MYL10* | 2.4 | *RPS27L* | 2.5 | *TLR3* | 6.0 |
| *BAI1* | 2.6 | *EMX1* | 2.9 | *IKBIP* | 3.8 | *MYO1A* | 5.6 | *RRM2B* | 4.2 | *TMEM151B* | 3.4 |
| *BBC3* | 7.2 | *EPB49* | 2.2 | *IL27* | 2.2 | *MYO7A* | 3.6 | *RSPO1* | 2.4 | *TMEM173* | 2.7 |
| *BBS9* | 7.9 | *EPN3* | 2.5 | *IL4I1* | 5.4 | *NACAD* | 2.5 | *RYR1* | 5.9 | *TMEM229B* | 2.7 |
| *BDKRB2* | 2.2 | *EPPK1* | 3.8 | *INPP5D* | 13.4 | *NADSYN1* | 4.0 | *S1PR4* | 4.0 | *TMEM40* | 2.8 |
| *BLNK* | 2.1 | *EPS8L2* | 4.7 | *ISG15* | 2.6 | *NDN* | 3.2 | *SAC3D1* | 2.2 | *TMEM52* | 2.4 |
| *BMP7* | 3.1 | *ERAP2* | 2.9 | *ISYNA1* | 2.9 | *NHLH2* | 2.8 | *SATB1* | 4.2 | *TMEM8B* | 2.7 |
| *BTG2* | 6.5 | *ERN2* | 2.2 | *ITGA4* | 2.6 | *NINJ1* | 4.2 | *SCARF2* | 2.3 | *TNFAIP8* | 2.7 |
| *C12orf45* | 2.1 | *ETV7* | 24.6 | *ITGB2* | 4.0 | *NLRP13* | 3.1 | *SCARNA9L* | 2.6 | *TNFRSF10C* | 26.5 |
| *C12orf5* | 2.2 | *EXD3* | 2.4 | *ITLN2* | 2.4 | *NLRX1* | 3.1 | *SCGB1D1* | 5.6 | *TNFRSF14* | 18.7 |
| *C14orf176* | 2.3 | *EXOC3L4* | 2.6 | *IZUMO1* | 3.7 | *NODAL* | 3.5 | *SCGB1D2* | 10.6 | *TNNC2* | 9.0 |
| *C16orf5* | 6.2 | *EYA1* | 4.3 | *IZUMO4* | 2.0 | *NOTCH1* | 2.1 | *PVT1* | 2.1 | *TNNI2* | 7.2 |
| *C17orf109* | 3.1 | *F10* | 2.0 | *KANK3* | 3.6 | *NPPC* | 4.0 | *PXDN* | 3.7 | *TP53* | 2.7 |
| *C17orf82* | 2.3 | *FAM167A* | 2.0 | *KCNB1* | 7.4 | *NPTX1* | 4.0 | *Q6TXG5* | 12.6 | *TP53I11* | 3.6 |
| *C1orf170* | 2.7 | *FAM183A* | 4.4 | *KCNF1* | 5.4 | *NR1I2* | 8.5 | *Q8E8P5* | 4.1 | *TP53I3* | 16.1 |

Table III. Continued.

| Gene | Fold induction | | | | | | | | | |
|---|---|---|---|---|---|---|---|---|---|---|
| *C1orf187* | 5.9 | *FAM183B* | 3.2 | *KCNIP2* | 2.0 | *NRG1* | 2.8 | *RAB37* | 4.4 | *TP53INP1* | 4.5 |
| *C1S* | 4.5 | *FAM184A* | 2.2 | *KCNJ12* | 3.8 | *NRG2* | 2.5 | *RABEPK* | 2.1 | *TPSD1* | 2.0 |
| *C20orf108* | 4.6 | *FAM198B* | 3.6 | *KCNK7* | 4.8 | *NRP2* | 2.9 | *RALGDS* | 2.8 | *TRANK1* | 2.5 |
| *C2orf88* | 2.8 | *FAM71B* | 4.7 | *KCTD11* | 2.3 | *NTN1* | 9.1 | *RASAL1* | 3.0 | *TREH* | 2.3 |
| *C3P1* | 2.9 | *FAM87B* | 3.8 | *KEL* | 19.5 | *NUAK2* | 2.6 | *RASGRF1* | 2.1 | *TREM2* | 12.2 |
| *C4B* | 3.8 | *FAM92B* | 3.9 | *KIAA0247* | 2.8 | *NUDT8* | 2.3 | *RASSF4* | 2.5 | *TREML1* | 5.0 |
| *C6orf154* | 2.2 | *FAS* | 4.0 | *KIAA1324* | 4.3 | *NUPR1* | 8.5 | *RD3* | 8.6 | *TRIM22* | 2.4 |
| *C9orf135* | 3.4 | *FBLIM1* | 2.7 | *KIAA1751* | 3.9 | *ODF3L1* | 4.5 | *REEP2* | 4.0 | *TRIM29* | 2.5 |
| *C9orf169* | 2.1 | *FBLN2* | 2.4 | *KLHL30* | 24.1 | *ODZ4* | 3.2 | *RET* | 2.5 | *TRIM55* | 2.3 |
| *CA12* | 2.8 | *FCER1A* | 2.2 | *KNDC1* | 2.8 | *ORAI3* | 3.0 | *RGL1* | 3.2 | *TRPM6* | 2.2 |
| *CACNA1I* | 2.1 | *FCGBP* | 2.5 | *KRT17* | 9.1 | *OSBPL7* | 2.3 | *RGS16* | 3.2 | *TRPV6* | 4.2 |
| *CAMK2B* | 3.1 | *FCHSD2* | 2.1 | *KRT5* | 10.3 | *OTP* | 5.1 | *RHOD* | 3.4 | *TSGA10* | 2.4 |
| *CARNS1* | 4.2 | *FCRLA* | 2.0 | *LACC1* | 2.0 | *P2RY2* | 2.0 | *RIC3* | 12.8 | *TSPAN10* | 3.4 |
| *CASP1* | 2.2 | *FDXR* | 4.3 | *LAMP3* | 5.1 | *PADI3* | 9.5 | *RIIAD1* | 2.4 | *TSPAN11* | 2.2 |
| *CASP10* | 3.7 | *FLG* | 11.0 | *LANCL3* | 2.2 | *PADI4* | 5.3 | *RIMBP3* | 2.1 | *TSPAN18* | 2.2 |
| *CASZ1* | 3.3 | *FLJ30838* | 2.1 | *LAPTM5* | 4.7 | *PARP10* | 4.1 | *RIMS4* | 3.1 | *UCN3* | 2.1 |
| *CBS* | 21.6 | *FLJ32255* | 7.7 | *LARGE* | 2.2 | *PCDHAC1* | 10.2 | *RIN1* | 2.8 | *UCP2* | 2.1 |
| *CCDC108* | 4.6 | *FLJ36000* | 2.3 | *LCE1B* | 10.3 | *PDE6C* | 5.4 | *RINL* | 2.3 | *UNC45B* | 2.5 |
| *CCDC144A* | 2.1 | *FLJ37786* | 2.3 | *LCE1C* | 45.4 | *PDGFRB* | 4.0 | *ROM1* | 2.3 | *UNC5B* | 2.1 |
| *CCDC3* | 3.5 | *FLJ41350* | 3.0 | *LCN15* | 25.1 | *PDYN* | 3.2 | *ROR1* | 2.6 | *USH1G* | 2.2 |
| *CD36* | 4.5 | *FLJ42969* | 2.1 | *LCN2* | 2.1 | *PHLDA3* | 5.5 | *RPS27L* | 2.5 | *USHBP1* | 2.2 |
| *CD72* | 4.2 | *FLJ43663* | 2.6 | *LDLRAD1* | 13.3 | *PHLDB3* | 2.2 | *RRM2B* | 4.2 | *USP29* | 3.1 |
| *CD79B* | 2.9 | *FLJ44896* | 22.6 | *LEMD1* | 3.3 | *PIDD* | 4.1 | *RSPO1* | 2.4 | *VIL1* | 6.8 |
| *CD82* | 6.7 | *FLT3LG* | 2.7 | *LGALS7* | 8.8 | *PKNOX2* | 2.3 | *RYR1* | 5.9 | *WDR63* | 7.0 |
| *CDH16* | 15.0 | *FOXP1* | 2.2 | *LGALS9* | 5.2 | *PLA2G4C* | 2.2 | *S1PR4* | 4.0 | *WNT11* | 4.0 |
| *CDKN1A* | 8.0 | *FP588* | 2.3 | *LGALS9C* | 12.8 | *PLA2G4D* | 6.6 | *SAC3D1* | 2.2 | *WNT4* | 4.4 |
| *CDSN* | 3.3 | *FRMPD2* | 2.2 | *LHFPL1* | 2.4 | *PLCL2* | 9.6 | *SATB1* | 4.2 | *WNT7A* | 3.8 |
| *CEACAM1* | 6.9 | *FXYD2* | 6.4 | *LINC00087* | 2.0 | *PLK3* | 3.4 | *SCARF2* | 2.3 | *WNT7B* | 3.3 |
| *CELA3B* | 2.1 | *FXYD3* | 3.9 | *LINC00320* | 2.1 | *PLK5* | 2.5 | *SCARNA9L* | 2.6 | *XG* | 2.9 |
| *CFTR* | 5.0 | *GABRE* | 3.6 | *LINC00324* | 2.0 | *PLXNB1* | 2.3 | *SCGB1D1* | 5.6 | *XLOC_004323* | 3.7 |
| *CGB* | 2.7 | *GADD45G* | 2.2 | *LOC100133669* | 4.5 | *PLXNB3* | 6.0 | *SCGB1D2* | 10.6 | *XLOC_011803* | 2.5 |
| *CHD2* | 2.2 | *GDF15* | 5.7 | *LOC100289026* | 8.4 | *PML* | 3.1 | *SCN3B* | 4.1 | *XLOC_l2_000159* | 3.7 |
| *CHGA* | 2.9 | *GGTLC1* | 2.1 | *LOC100506305* | 2.1 | *PNLIPRP2* | 5.1 | *SDPR* | 4.3 | *XLOC_l2_010751* | 8.0 |
| *CHI3L2* | 2.4 | *GGTLC2* | 2.6 | *LOC151760* | 3.0 | *PODXL* | 3.3 | *SEMA3B* | 4.3 | *XLOC_l2_014832* | 2.1 |
| *CHRNA6* | 3.0 | *GH1* | 3.2 | *LOC283050* | 2.5 | *POLH* | 2.9 | *SEMA3F* | 2.9 | *XPC* | 2.5 |
| *CKM* | 4.5 | *GH2* | 15.1 | *LOC283710* | 5.7 | *POU2AF1* | 4.5 | *SERPINA11* | 2.3 | *ZMAT3* | 4.2 |
| *CLCA2* | 6.0 | *GIMAP5* | 2.3 | *LOC284837* | 2.1 | *POU3F2* | 2.6 | *SERPINB4* | 2.6 | *ZNF658* | 2.2 |
| *CMBL* | 3.6 | *GJD3* | 6.1 | *LOC285548* | 2.1 | *PPY* | 2.9 | *SERPINB5* | 2.3 | *ZNF664-FAM101A* | 3.3 |
| *CMKLR1* | 2.8 | *GLIPR2* | 2.1 | *LOC375295* | 2.3 | *PPY2* | 2.3 | *SERPINE1* | 3.1 | *ZNF69* | 2.8 |
| *COBLL1* | 2.2 | *GLS2* | 3.7 | *LOC388242* | 3.3 | *PRAMEF3* | 2.1 | *SESN1* | 5.5 | *ZNF850* | 2.3 |
| *COL17A1* | 4.0 | *GMFG* | 2.1 | *LOC388780* | 4.0 | *PRDM1* | 8.8 | *SH3TC1* | 2.1 | | |

for samples used for mass spectrometry). Cells without ADR treatment were used as controls.

We identified 124 candidates on the basis of the proteome analysis at f1 >2 ($p<0.05$, Table II) and 523 candidates on the basis of the transcriptome analysis at f2 >2 ($p<0.05$, Table III). Ultimately, we identified 28 genes through mass spectrometry and microarray screening.

We then further screened these 28 genes by using a TCGA dataset consisting of 624 colorectal tumor samples. We selected genes as follows; i) significantly ($p<0.05$) higher expression in normal colon tissues than in tumor tissues and ii) significantly ($p<0.05$) higher expression in tumor tissues with wild-type *p53* than in tissues with mutant *p53* (Fig. 1).

As a result, two novel p53 targets (MICALL1 and APOBEC3C) and three known p53 targets (CDKN1A, FAS, TP53I3) were identified in our screening (Fig. 1B). Among the two novel candidates, induction of MICALL1 was validated by both qPCR and western blotting (Fig. 2A and B). Therefore,

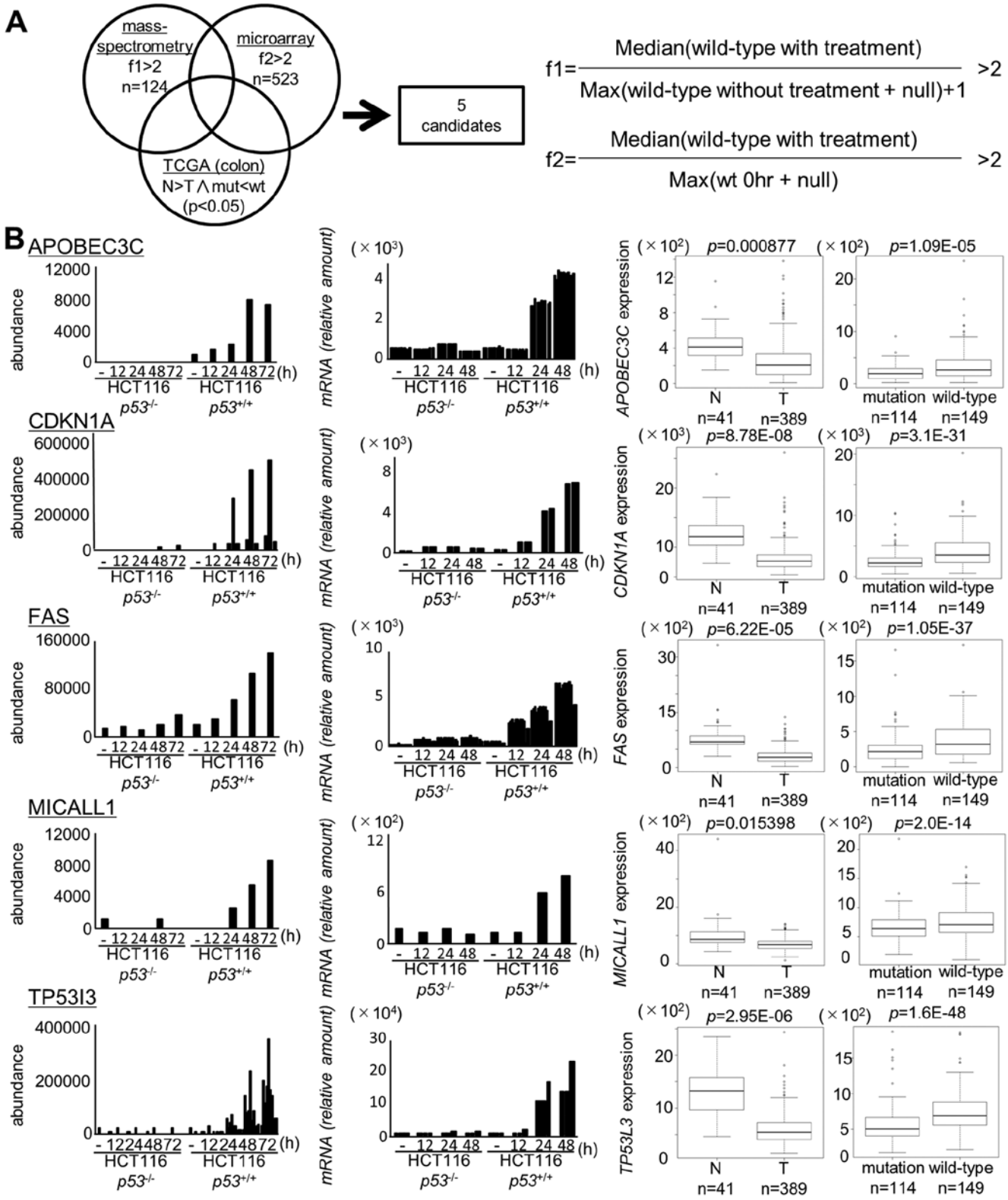


Figure 1. MICALL1 is a p53 downstream target. (A) The analysis framework for identifying candidate genes. HCT116 $p53^{+/+}$ and HCT116 $p53^{-/-}$ cells were harvested at the indicated times after 2 $\mu$g/ml adriamycin (ADR) treatment for 2 h. Whole cell lysate samples were subjected to mass spectrometry and DNA microarrays. These data as well as TCGA colorectal data were analyzed. Two novel p53 targets and three known p53 targets were identified by the screening. (B) Screening data of candidates (including three previously reported candidates). (Left) Mass spectrometry data. (Middle) Microarray data. (Right) Box plot of candidate expression in colorectal adenocarcinoma tissues using TCGA data. The top bar of the box is the upper or third quartile; the bottom bar of the box is the lower or first quartile; the middle bar is the median value. P-values were calculated with Mann-Whitney U tests.

we selected MICALL1 for further analysis. We also found that MICALL1 was induced in H1299 cells infected by Ad-p53 but not in Ad-LacZ-infected cells (Fig. 2C).

To evaluate the effect of p53 activation on MICALL1 expression, we analyzed the expression of MICALL1 using HCT116 cells treated with Nutlin-3a (inhibitor of MDM2) that

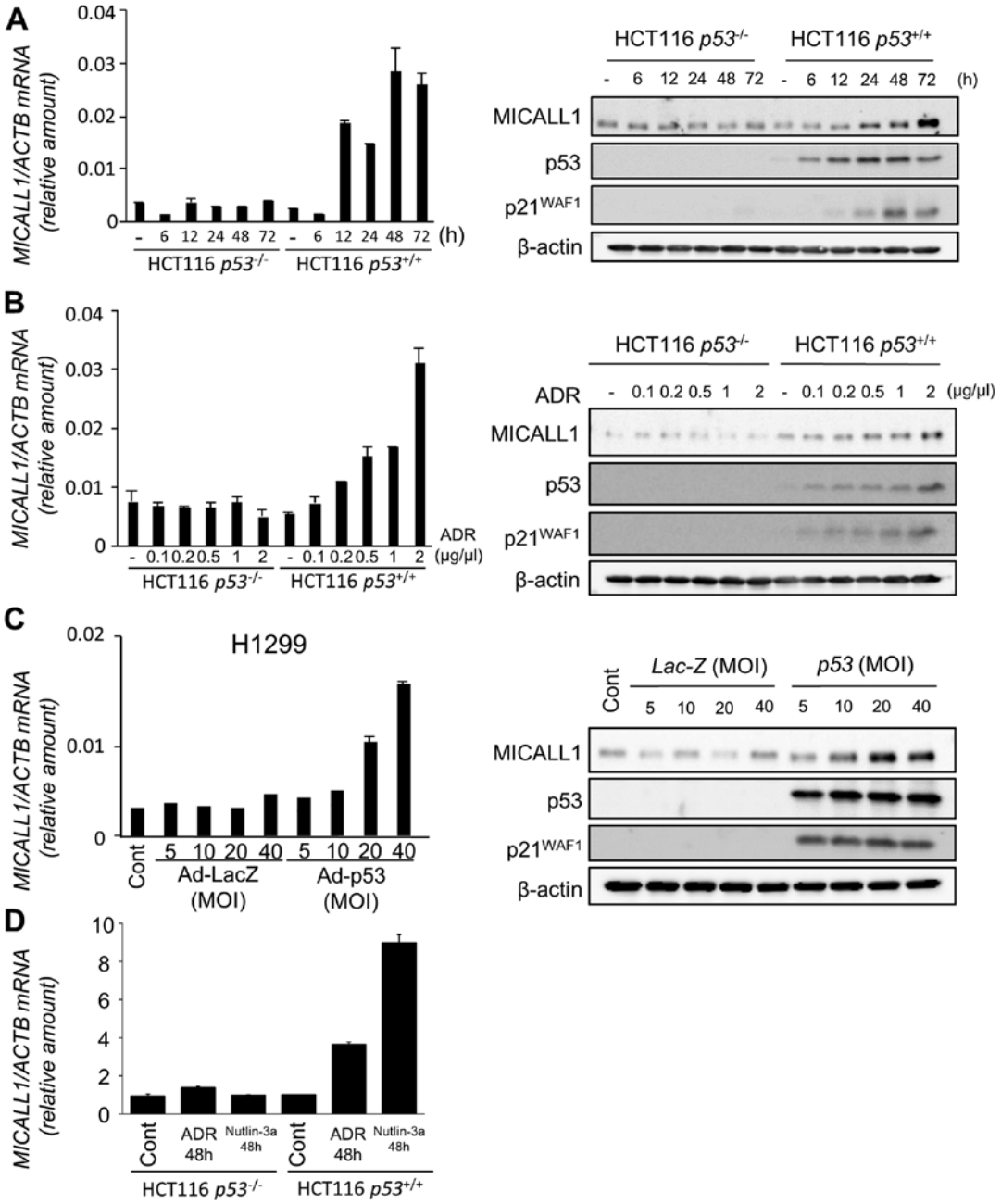


Figure 2. Induction of MICALL1 by DNA damage and p53. (A) (Left panel) Quantitative real-time PCR (qPCR) analysis of MICALL1 in HCT116 *p53*$^{-/-}$ or *p53*$^{+/+}$ cells harvested at the indicated times after 2 μg/ml adriamycin (ADR) treatment for 2 h. β-actin was used for normalization of expression levels. Error bars represent the SD (n=2). (Right panel) HCT116 *p53*$^{-/-}$ or HCT116 *p53*$^{+/+}$ cells were treated with 2 μg/ml ADR for 2 h. At the indicated times after treatment, whole cell extracts were subjected to western blot analysis using an anti-MICALL1, anti-p53, anti-p21, or anti-β-actin antibody. (B) (Left panel) qPCR analysis of MICALL1 in HCT116 *p53*$^{-/-}$ or *p53*$^{+/+}$ cells harvested at 48 h after the indicated concentration of ADR treatment for 2 h. β-actin was used for normalization of expression levels. Error bars represent the SD (n=2). (Right panel) HCT116 *p53*$^{-/-}$ or HCT116 *p53*$^{+/+}$ cells were treated with the indicated concentration of ADR for 2 h. After 48 h of treatment, whole cell extracts were subjected to western blot analysis using an anti-MICALL1, anti-p53, anti-p21, or anti-β-actin antibody. (C) (Left panel) qPCR analysis of MICALL1 in H1299 (p53 null) cells infected with adenovirus expressing p53 (Ad-p53) or LacZ (Ad-LacZ) at MOIs from 5 to 40. (Right panel) H1299 cells infected with Ad-p53 or Ad-LacZ at MOIs from 5 to 40. At 36 h after treatment, whole cell extracts were subjected to western blot analysis with an anti-MICALL1, anti-p53, anti-p21, or anti-β-actin antibody. (D) qPCR analysis of MICALL1 in HCT116 *p53*$^{-/-}$ or *p53*$^{+/+}$ cells harvested at 48 h after 0.5 μM ADR or 10 μM nutlin-3a treatment for 2 h. β-actin was used for normalization of expression levels. Error bars represent the SD (n=2).

activates p53. As shown in Fig. 2D, MICALL1 expression was induced by Nutrin-3a only in HCT116 *p53*$^{+/+}$ cells. These results clearly indicate that MICALL1 is induced by p53 activation.

We then performed immunocytochemical analysis using HCT116 *p53*$^{+/+}$ and *p53*$^{-/-}$ cells under ADR treatment (Fig. 3). Without ADR treatment, expression of MICALL1 was very low in both types of cells. However, in response to ADR treatment, MICALL1 was induced at the cytoplasmic tubular structure only in HCT116 *p53*$^{+/+}$ cells.

*MICALL1 is a direct target of p53*. To investigate whether MICALL1 is a direct target of p53, we searched for the p53

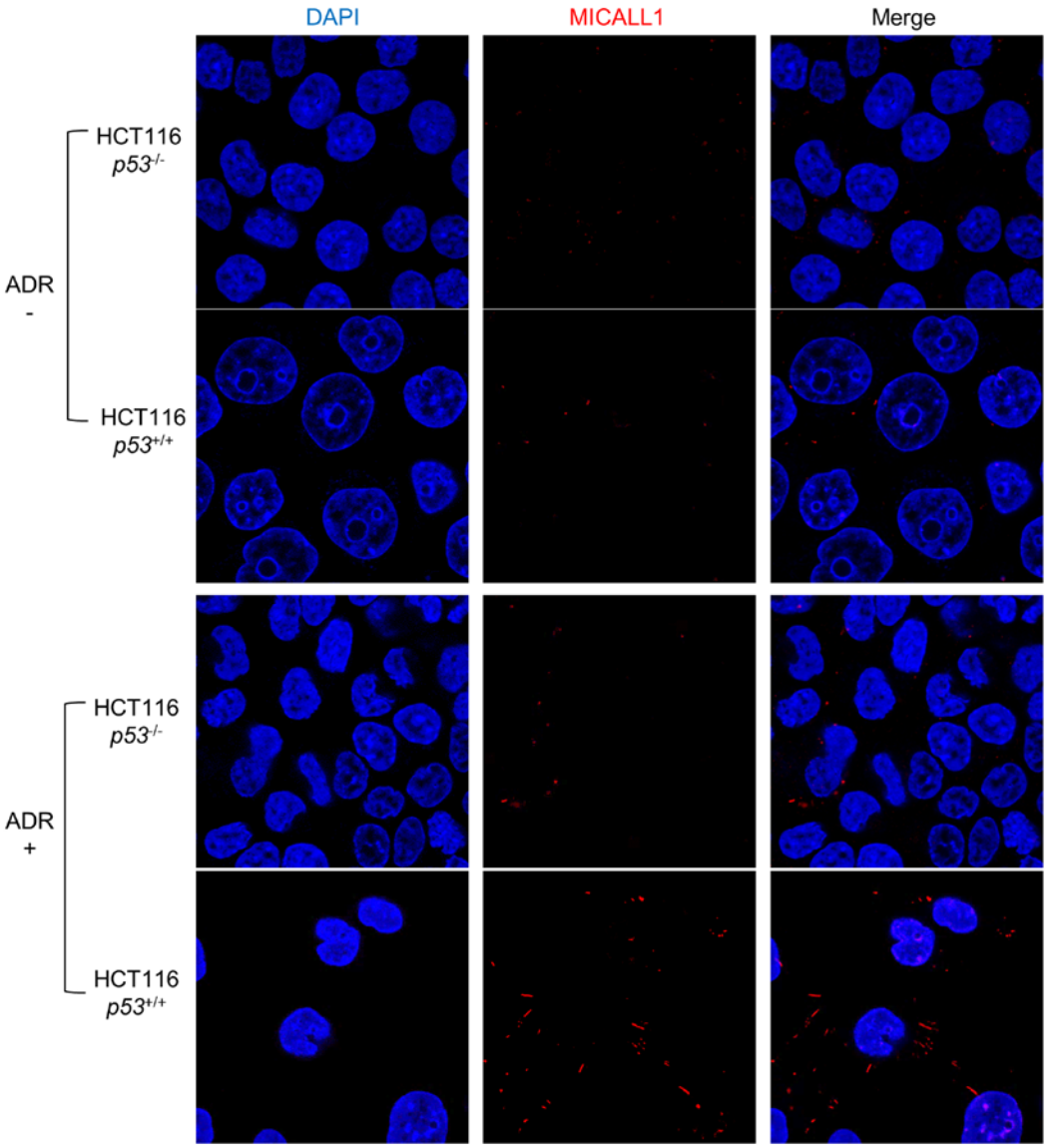


Figure 3. Localization of MICALL1 in HCT116 $p53^{+/+}$ and $p53^{-/-}$ cells. HCT116 $p53^{+/+}$ and $p53^{-/-}$ cells were grown on cover slips and treated with 2 $\mu$g/ml Adriamycin for 2 h. At 48 h after ADR treatment, cells were then fixed, and MICALL1 was detected using a monoclonal anti-MICALL1 antibody followed by an anti-mouse antibody.

binding motif (16) within the *MICALL1* locus and found two potential binding sequences (p53BS1, p53BS2) in the approximately 3000 base pair of 5' flanking sequence (Fig. 4A). A 151-base pair DNA fragment (p53BS1+2) including two p53 binding sequences was amplified and cloned upstream of the minimal promoter in the pGL4.24 vector (pGL4.24/p53BS1+2). The reporter assays showed increased luciferase activity in H1299 cells transfected with pGL4.24/p53BS1+2 in the presence of a plasmid expressing wild-type p53 (Fig. 4B). However, base substitutions in p53BS (pGL4.24/p53BSmut1, pGL4.24/p53BSmut2) decreased the observed enhanced luciferase activity.

To verify whether p53 directly bound to p53BS, we performed a ChIP assay using H1299 cells infected with either Ad-p53 or Ad-LacZ. After precipitation with an anti-p53 antibody, the DNA fragment containing p53BS1 was quantified by qPCR, which showed that p53 specifically bound to p53BS1 in cells infected with Ad-p53 (Fig. 4C). Thus, we concluded that p53 regulates *MICALL1* expression through p53BS in the 5' flanking region of the *MICALL1* gene.

*Role of MICALL1 in the p53 pathway*. To further investigate the role of MICALL1 as a p53 downstream target, we screened MICALL1-interacting proteins by LC-MS analysis. MICALL1 was immunoprecipitated from cell lysates of HEK293T cells transfected with the MICALL1 expression plasmid. The protein complex including immunopurified MICALL1 was analyzed by SDS-PAGE and subsequent silver staining. A protein band at approximately 75 kDa, which was abundant in the protein complex including MICALL1, was subjected to LC-MS analysis. The results indicated that CD2AP is likely to bind MICALL1 (Fig. 5A and B). Interaction between CD2AP and MICALL1 was confirmed by western blotting (Fig. 5C). We also confirmed the interaction by using lysates from HEK293T cells overexpressing FLAG-MICALL1 and HA-CD2AP. Moreover, this interaction between endogenous

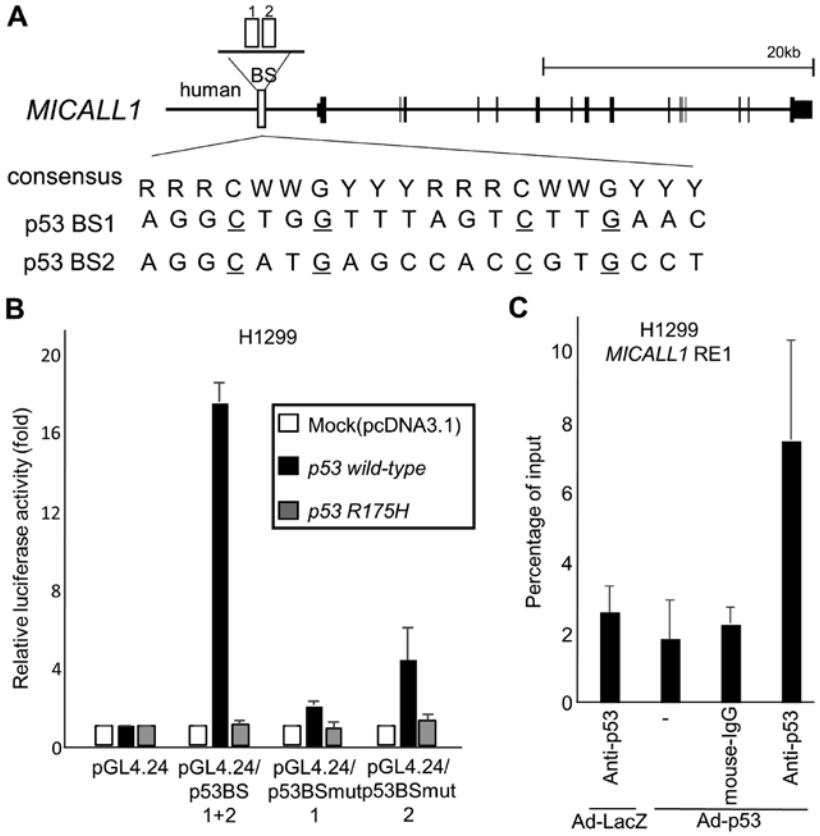


Figure 4. MICALL1 is a direct p53 target. (A) Genomic structure of the *MICALL1* gene. The white boxes indicate the location of the potential p53 binding sequence (p53BS1, 2). Comparison of p53BS1 and 2 with the consensus p53 binding sequence. R, purine; W, A or T; Y, pyrimidine. Nucleotides identical to the consensus sequence are shown in capital letters. The underlined cytosines and guanines were substituted for thymines to examine the specificity of the p53 binding sequence. (B) Results of luciferase assays for the genomic fragment containing p53BS with or without substitutions in the motif. Luciferase activity is indicated relative to the activity of the vector alone, with the SD (n=3). In this study, H1299 cells are transfected with reporter plasmid designated as (1) pGL4.24, (2) pGL4.24/p53BS1+2, (3) pGL4.24/p53BSmut1, or (4) pGL4.24/p53BSmut2 together with pcDNA3.1, plasmid expression wild-type p53 or R175H mutant p53. pGL4.74 is also cotransfected for normalization of transfection efficiency. H1299 cells were not treated with Adriamycin. (C) A ChIP assay was performed using H1299 cells infected at an MOI of 10 with Ad-p53 (lanes 2-4) or Ad-LacZ (lane 1). H1299 cells were not treated with Adriamycin. DNA-protein complexes were immunoprecipitated with an anti-p53 antibody (lanes 1 and 4) and then subjected to qPCR analysis to evaluate the amount of genomic fragments containing the p53 binding sequence in *MICALL1*. Immunoprecipitates pulled down with an anti-IgG antibody (lane 3) or in the absence of antibody (-) (lane 4) were used as negative controls. Columns, mean; error bars, SD (n=3).

MICALL1 protein and CD2AP was observed in ADR-treated HCT116 cells (Fig. 5D).

*Regulation of tubular recycling endosomes (TREs) by the p53-MICALL1 pathway*. MICALL1 has been reported to be a marker of TREs, which are essential for the recycling of receptors and lipids to the plasma membrane (20). MICALL1 has also been reported to recruit RAB8A, a protein related to vesicle-mediated transport, to TREs (21). Since MICALL1 was found at tubular structure in the cytoplasm after DNA damage, we investigated the subcellular localization of CD2AP and RAB8A in HCT116 $p53^{+/+}$ cells (Fig. 6A and B).

Initially, we determined the localization of CD2AP and RAB8A after DNA damage. HCT116 $p53^{+/+}$ cells were grown on coverslips and treated with 2 $\mu$g/ml ADR; 48 h later, CD2AP and RAB8A exhibited a tubular-like distribution with MICALL1 (Fig. 6A-1, 2, and B-1, 2). Thus, CD2AP and RAB8A exhibited altered cytoplasmic localization to TREs after DNA damage.

Next, we tested whether p53 or MICALL1 knockdown changed the localization of CD2AP and RAB8A after DNA damage (Fig. 6C). At 48 h after ADR treatment, cells were fixed, and MICALL1 and CD2AP or RAB8A was identified with antibodies. According to the results, their localization change did not occur in p53 or MICALL1-knockdown cells (Fig. 6A-4, 5, 6, and B-4, 5, 6). According to the above results, MICALL1 is involved in TRE regulation in the response to DNA damage.

*MICALL1 and CD2AP regulate cell proliferation*. To investigate the role of MICALL1 in cell proliferation, we performed a colony formation assay using HCT116 cells and found a significant decrease in colony counts for cells transfected with MICALL1 compared with cells mock transfected with the vector (Fig. 6D). Furthermore, ectopic expression of CD2AP also repressed cell growth like MICALL1 expressing cells (Fig. 6D). These results indicated that MICALL1 would suppress tumor cell growth through the regulation of CD2AP.

## Discussion

In this study, we identified MICALL1 as a novel p53 downstream target by using multi-omics analysis. Moreover, we identified CD2AP as a protein that interacts with MICALL1.

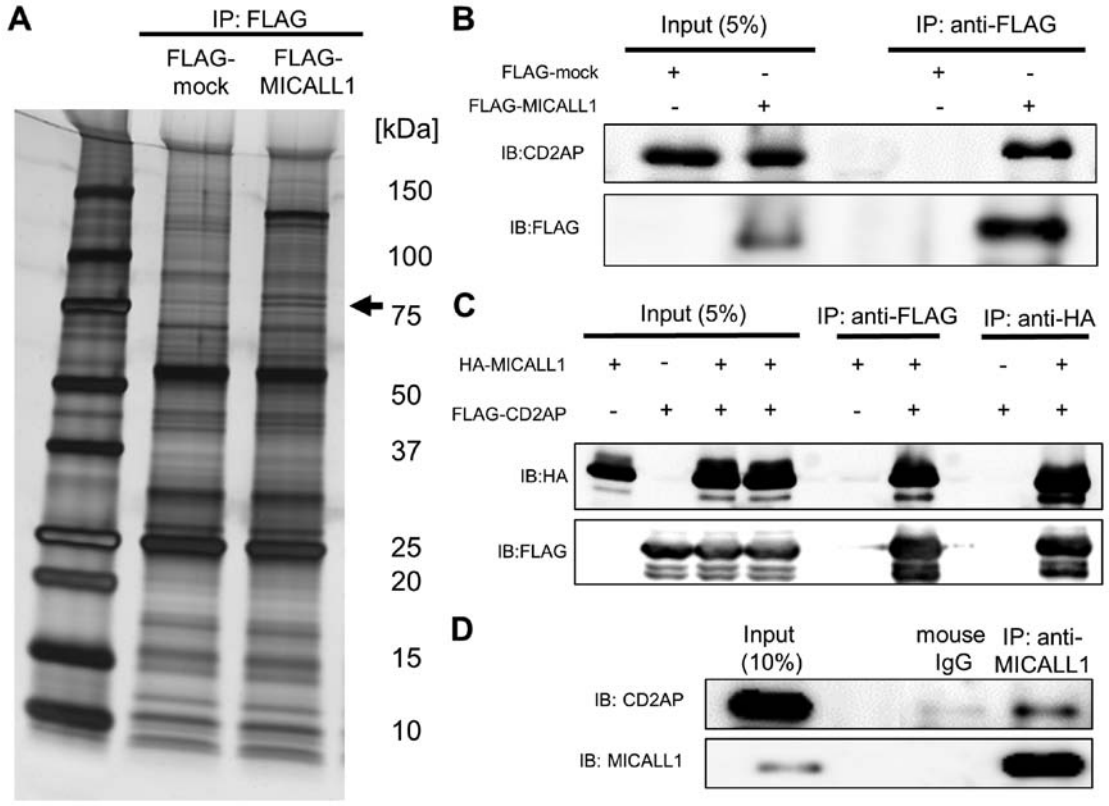


Figure 5. MICALL1 binds to CD2AP. (A) Silver staining. HEK293T cells were transfected with FLAG-mock and FLAG-MICALL1, and the samples were immunoprecipitated with anti-FLAG followed by G-Sepharose beads. Silver staining was then performed. Briefly, gels were fixed with 40% ethanol/10% acetic acid for 20 min. After several changes of 30% ethanol and water, the gels were sensitized by incubation in silver nitrate for 10 min and thorough rinsing with water. The gels were developed with developing solution, and the reaction was terminated with stop solution. All gel bands were stored at -20˚C prior to mass spectrometry. HEK293T cells were not treated with Adriamycin (A-C). (B) Western blotting for confirmation. Using the samples as in (A), the blots were probed with anti-CD2AP and anti-FLAG antibodies, as indicated. (C) Immunoprecipitation of ectopically expressed MICALL1-CD2AP complex. HEK293T cells were transfected with HA-MICALL1 and FLAG-CD2AP. MICALL1 and CD2AP were immunoprecipitated with anti-HA or anti-FLAG, respectively, followed by G-Sepharose beads; blots were probed with anti-HA or anti-FLAG, as indicated. The data shown are representative of two independent experiments. (D) Immunoprecipitation of endogenous MICALL-CD2AP complex. HCT116 $p53^{+/+}$ cells were treated with 2 $\mu$g/ml Adriamycin. MICALL1 and CD2AP were immunoprecipitated with anti-MICALL1, followed by G-sepharose beads; blots were probed with anti-MICALL1 or anti-CD2AP, as indicated. The data shown are representative of two independent experiments.

In response to DNA damage, MICALL1, CD2AP, and RAB8A co-localize at tubular-like structures in the cytoplasm in a p53-dependent manner.

Endocytosis, a process that transports materials such as membrane proteins to membrane vesicles, regulates cell signaling to adjust receptor trafficking (22) and has many functions in cell migration, polarity, adhesion, differentiation, apoptosis, and autophagy (23-25). Endocytosis is also dysregulated in cancer. For example, HER2 inhibits endocytic degradation of CXCR4 and induce lung metastasis in breast cancer (26). Moreover, Rab25 changes the localization of integrin and consequently enhances invasion of cancer cells (27).

TREs are related to 'slow-recycling' (28). MICALL1 was identified as a member of a family of proteins that interact with the focal adhesion plaque protein CasL (29). MICALL1 and Syndapin2 promote tubulation of recycling endosomes with phosphatidic acid (PA) and elongate tubules to the plasma membrane (20). MICALL1 also guides EHD1 to TREs (12) and regulates mitosis with EHD1 (30). Thus, MICALL1 is considered to be a regulator of TREs (12). However, the role of MICALL1 in colorectal cancer has not been reported to date.

We found that ectopic expression of MICALL1 significantly inhibited the proliferation of HCT116 colorectal cancer cells. *MICALL1* expression is suppressed in colorectal cancer with *p53* mutations (Fig. 1B). Moreover, the p53-MICALL1 pathway is essential for translocation of CD2AP to TREs in response to DNA damage. CD2AP was identified as a scaffold protein expressed on the surface of T-lymphocytes and antigen-presenting cells, and it regulates receptor trafficking among endosomes as an effector of the small GTPase Rab4 (31). Furthermore, CD2AP promotes EGFR degradation with Cbl (32), and MICALL1 has also been shown to retain EGFR in late endosome (33). Although the relationship between TREs and cancer is not yet clear, the p53-MICALL1 pathway appears to exert an antitumor effect via regulation of receptor trafficking.

Several endosomal proteins, such as CAV1, TSAP6, CHMP4C and DRAM1, have previously been shown to be p53 targets (24,25,34,35). However, the role of p53 in recycling endosomes has not been reported. Although the molecular mechanism by which MICALL1 regulates colorectal tumor cell growth should be elucidated in the future, our findings indicate the regulation of TREs occurs through the p53-MICALL1 pathway.

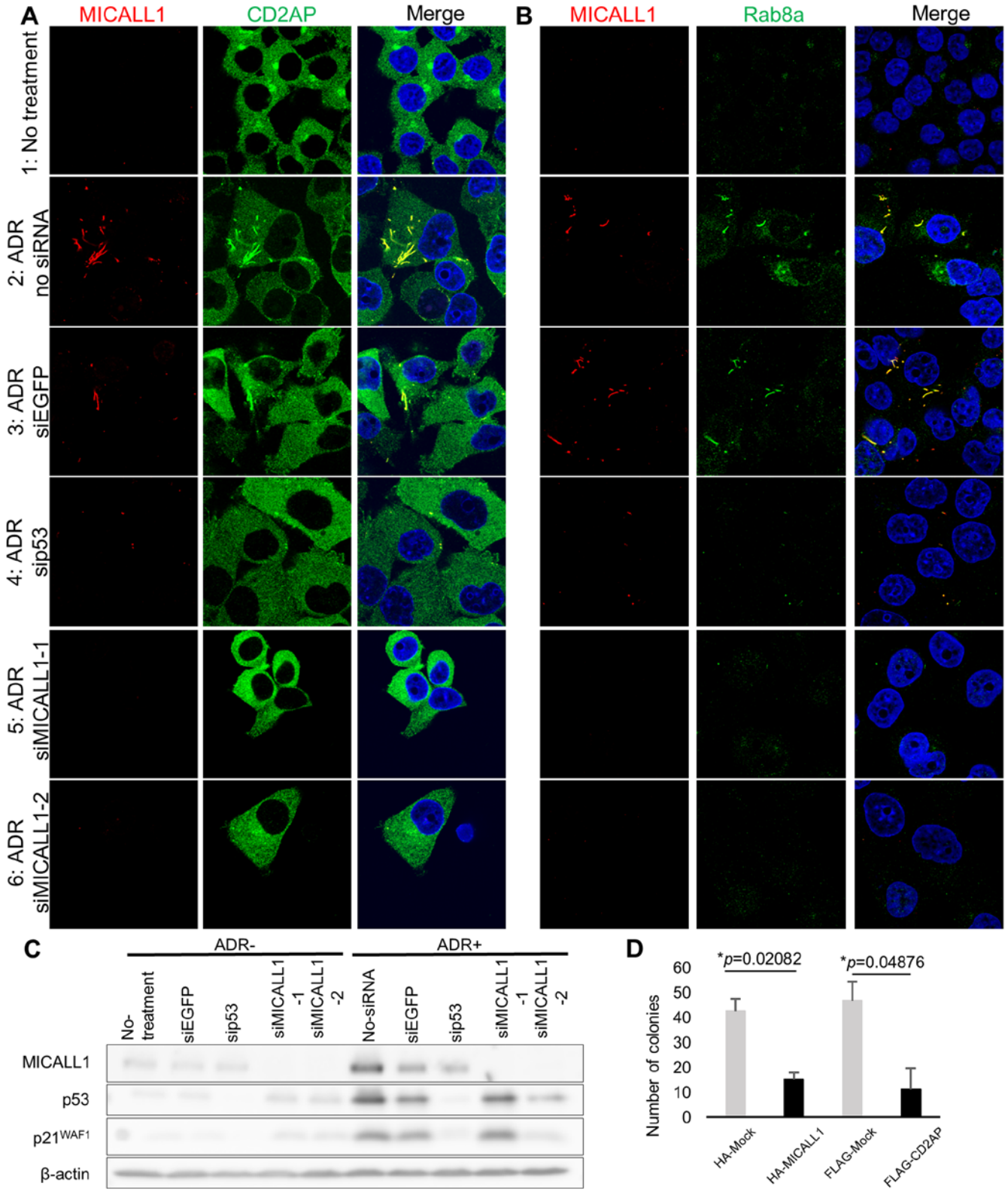


Figure 6. MICALL1 colocalizes with RAB8A and CD2AP. (A) HCT116 *p53*$^{+/+}$ cells were grown on cover slips and transiently transfected with siMICALL1, si-EGFP or si-p53. Cells were treated with 2 $\mu$g/ml of ADR for 2 h and then incubated in normal medium for 48 h. The cells were then fixed, and MICALL1 and CD2AP were identified with a monoclonal anti-MICALL1 antibody followed by an anti-mouse IgG antibody; endogenous CD2AP was identified with an anti-CD2AP antibody followed by an anti-rabbit IgG antibody. (B) HCT116 *p53*$^{+/+}$ cells were grown on cover slips and transiently transfected with siMICALL1, si-EGFP or si-p53. The cells were treated with 2 $\mu$g/ml of ADR for 2 h and then incubated in normal medium for 48 h. The cells were then fixed, and MICALL1 and RAB8A were detected by a monoclonal anti-MICALL1 antibody followed by an anti-mouse antibody; endogenous RAB8A was identified with an anti-RAB8A antibody followed by an anti-rabbit antibody. (C) HCT116 *p53*$^{+/+}$ cells grown in 100-mm dishes were either mock treated or treated with siRNA against EGFP, p53, and MICALL1. The cells were treated with 2 $\mu$g/ml of ADR for 2 h and then incubated in normal medium for 48 h. After lysis, proteins were separated by SDS-PAGE, transferred to nitrocellulose membranes and immunoblotted with anti-MICALL1, anti-p53, anti-p21 and anti-β-actin antibodies. (D) Colony formation by HCT116 cells. Expression of MICALL1 blocked the growth and colony counts of HCT116 cells; colony formation was measured using a colony formation assay. The number of colonies was counted at 11-20 days after transfection. Values are the averages ± SDs of duplicate experiments.

## Acknowledgements

We thank S. Takahashi, M. Oshima, S. Oda and A. Sei for assistance with various techniques. We also thank the Cancer Genome Atlas (TCGA) project and members of Cancer Genomics Hub (CGHub) for making all TCGA data publicly accessible. This work was supported in part by a grant from the Japan Society for the Promotion of Science and the Ministry of Education, Culture, Sports, Science and Technology of Japan to K.M. and C.T., a grant from the Japan Agency for Medical Research and Development to K.M. and C.T., a grant from the Ministry of Health, Labor and Welfare of Japan to K.M., and a grant from the Takeda Science Foundation to K.M. and C.T.

## References

1. Bieging KT, Mello SS and Attardi LD: Unravelling mechanisms of p53-mediated tumour suppression. Nat Rev Cancer 14: 359-370, 2014.
2. Li T, Kon N, Jiang L, Tan M, Ludwig T, Zhao Y, Baer R and Gu W: Tumor suppression in the absence of p53-mediated cell-cycle arrest, apoptosis, and senescence. Cell 149: 1269-1283, 2012.
3. Fitzmaurice C, Dicker D, Pain A, Hamavid H, Moradi-Lakeh M, MacIntyre MF, Allen C, Hansen G, Woodbrook R, Wolfe C, *et al*; Global Burden of Disease Cancer Collaboration: The Global Burden of Cancer 2013. JAMA Oncol 1: 505-527, 2015.
4. Bailey CE, Hu CY, You YN, Bednarski BK, Rodriguez-Bigas MA, Skibber JM, Cantor SB and Chang GJ: Increasing disparities in the age-related incidences of colon and rectal cancers in the United States, 1975-2010. JAMA Surg 150: 17-22, 2015.
5. Fearon ER and Vogelstein B: A genetic model for colorectal tumorigenesis. Cell 61: 759-767, 1990.
6. Leslie A, Carey FA, Pratt NR and Steele RJ: The colorectal adenoma-carcinoma sequence. Br J Surg 89: 845-860, 2002.
7. Munro AJ, Lain S and Lane DP: P53 abnormalities and outcomes in colorectal cancer: A systematic review. Br J Cancer 92: 434-444, 2005.
8. Russo A, Bazan V, Iacopetta B, Kerr D, Soussi T and Gebbia N; TP53-CRC Collaborative Study Group: The TP53 colorectal cancer international collaborative study on the prognostic and predictive significance of p53 mutation: Influence of tumor site, type of mutation, and adjuvant treatment. J Clin Oncol 23: 7518-7528, 2005.
9. Krieg AJ, Hammond EM and Giaccia AJ: Functional analysis of p53 binding under differential stresses. Mol Cell Biol 26: 7030-7045, 2006.
10. Hammond EM, Mandell DJ, Salim A, Krieg AJ, Johnson TM, Shirazi HA, Attardi LD and Giaccia AJ: Genome-wide analysis of p53 under hypoxic conditions. Mol Cell Biol 26: 3492-3504, 2006.
11. Tanikawa C, Zhang YZ, Yamamoto R, Tsuda Y, Tanaka M, Funauchi Y, Mori J, Imoto S, Yamaguchi R, Nakamura Y, *et al*: The transcriptional landscape of p53 signalling pathway. EBioMedicine 20: 109-119, 2017.
12. Sharma M, Giridharan SS, Rahajeng J, Naslavsky N and Caplan S: MICAL-L1 links EHD1 to tubular recycling endosomes and regulates receptor recycling. Mol Biol Cell 20: 5181-5194, 2009.
13. Funauchi Y, Tanikawa C, Yi Lo PH, Mori J, Daigo Y, Takano A, Miyagi Y, Okawa A, Nakamura Y and Matsuda K: Regulation of iron homeostasis by the p53-ISCU pathway. Sci Rep 5: 16497, 2015.
14. Ueda K, Ishikawa N, Tatsuguchi A, Saichi N, Fujii R and Nakagawa H: Antibody-coupled monolithic silica microtips for highthroughput molecular profiling of circulating exosomes. Sci Rep 4: 6232, 2014.
15. Kanda Y: Investigation of the freely available easy-to-use software 'EZR' for medical statistics. Bone Marrow Transplant 48: 452-458, 2013.
16. el-Deiry WS, Kern SE, Pietenpol JA, Kinzler KW and Vogelstein B: Definition of a consensus binding site for p53. Nat Genet 1: 45-49, 1992.
17. Tanikawa C, Matsuda K, Fukuda S, Nakamura Y and Arakawa H: p53RDL1 regulates p53-dependent apoptosis. Nat Cell Biol 5: 216-223, 2003.
18. Mori J, Tanikawa C, Funauchi Y, Lo PH, Nakamura Y and Matsuda K: Cystatin C as a p53-inducible apoptotic mediator that regulates cathepsin L activity. Cancer Sci 107: 298-306, 2016.
19. Miyamoto T, Lo PHY, Saichi N, Ueda K, Hirata M, Tanikawa C and Matsuda K: Argininosuccinate synthase 1 is an intrinsic Akt repressor transactivated by p53. Sci Adv 3: e1603204, 2017.
20. Giridharan SS, Cai B, Vitale N, Naslavsky N and Caplan S: Cooperation of MICAL-L1, syndapin2, and phosphatidic acid in tubular recycling endosome biogenesis. Mol Biol Cell 24: 1776-1790, S1-15, 2013.
21. Rahajeng J, Giridharan SS, Cai B, Naslavsky N and Caplan S: MICAL-L1 is a tubular endosomal membrane hub that connects Rab35 and Arf6 with Rab8a. Traffic 13: 82-93, 2012.
22. Conn PM: Methods in Enzymology. G protein coupled receptors trafficking and oligomerization. Preface. Methods Enzymol 521: xix, 2013.
23. Sigismund S, Confalonieri S, Ciliberto A, Polo S, Scita G and Di Fiore PP: Endocytosis and signaling: Cell logistics shape the eukaryotic cell plan. Physiol Rev 92: 273-366, 2012.
24. Yu X, Riley T and Levine AJ: The regulation of the endosomal compartment by p53 the tumor suppressor gene. FEBS J 276: 2201-2212, 2009.
25. Crighton D, Wilkinson S, O'Prey J, Syed N, Smith P, Harrison PR, Gasco M, Garrone O, Crook T and Ryan KM: DRAM, a p53-induced modulator of autophagy, is critical for apoptosis. Cell 126: 121-134, 2006.
26. Li YM, Pan Y, Wei Y, Cheng X, Zhou BP, Tan M, Zhou X, Xia W, Hortobagyi GN, Yu D, *et al*: Upregulation of CXCR4 is essential for HER2-mediated tumor metastasis. Cancer Cell 6: 459-469, 2004.
27. Caswell PT, Spence HJ, Parsons M, White DP, Clark K, Cheng KW, Mills GB, Humphries MJ, Messent AJ, Anderson KI, *et al*: Rab25 associates with alpha5beta1 integrin to promote invasive migration in 3D microenvironments. Dev Cell 13: 496-510, 2007.
28. Jović M, Kieken F, Naslavsky N, Sorgen PL and Caplan S: Eps15 homology domain 1-associated tubules contain phosphatidylinositol-4-phosphate and phosphatidylinositol-(4,5)-bisphosphate and are required for efficient recycling. Mol Biol Cell 20: 2731-2743, 2009.
29. Suzuki T, Nakamoto T, Ogawa S, Seo S, Matsumura T, Tachibana K, Morimoto C and Hirai H: MICAL, a novel CasL interacting molecule, associates with vimentin. J Biol Chem 277: 14933-14941, 2002.
30. Reinecke JB, Katafiasz D, Naslavsky N and Caplan S: Novel functions for the endocytic regulatory proteins MICAL-L1 and EHD1 in mitosis. Traffic 16: 48-67, 2015.
31. Cormont M, Metón I, Mari M, Monzo P, Keslair F, Gaskin C, McGraw TE and Le Marchand-Brustel Y: CD2AP/CMS regulates endosome morphology and traffic to the degradative pathway through its interaction with Rab4 and c-Cbl. Traffic 4: 97-112, 2003.
32. Dikic I: CIN85/CMS family of adaptor molecules. FEBS Lett 529: 110-115, 2002.
33. Abou-Zeid N, Pandjaitan R, Sengmanivong L, David V, Le Pavec G, Salamero J and Zahraoui A: MICAL-like1 mediates epidermal growth factor receptor endocytosis. Mol Biol Cell 22: 3431-3441, 2011.
34. Bist A, Fielding CJ and Fielding PE: p53 regulates caveolin gene transcription, cell cholesterol, and growth by a novel mechanism. Biochemistry 39: 1966-1972, 2000.
35. Amson RB, Nemani M, Roperch JP, Israeli D, Bougueleret L, Le Gall I, Medhioub M, Linares-Cruz G, Lethrosne F, Pasturaud P, *et al*: Isolation of 10 differentially expressed cDNAs in p53-induced apoptosis: Activation of the vertebrate homologue of the drosophila seven in absentia gene. Proc Natl Acad Sci USA 93: 3953-3957, 1996.